

Angular analysis of polarized top quark decay into B-mesons in two different helicity systems

S. M. Moosavi Nejad^{a,b}, Mahboobe Balali^a

^a*Faculty of Physics, Yazd University, P.O. Box 89195-741, Yazd, Iran*

^b*School of Particles and Accelerators, Institute for Research in Fundamental Sciences (IPM), P.O.Box 19395-5531, Tehran, Iran*

E-mail: mmoosavi@yazd.ac.ir

ABSTRACT: We calculate the $\mathcal{O}(\alpha_s)$ radiative corrections to the spin dependent differential decay rates of the process $t \rightarrow b + W^+$. These are needed to study the angular distribution of the energy of hadrons produced in polarized top quark decays at next-to-leading order (NLO). In our previous work, we studied the angular distribution of the scaled-energy of bottom-flavored hadrons (B) from polarized top quark decays, using a specific helicity coordinate system where the top quark spin was measured relative to the bottom momentum (system 1). Here, we study the angular distribution of the energy spectrum of B-hadron in a different helicity system, where the top spin is specified relative to the W-momentum (system 2). These energy distributions are governed by the polarized and unpolarized rate functions which are related to the density matrix elements of the decay $t \rightarrow W^+ + b$. Through this paper, we present our predictions of the B-hadron spectrum in the polarized and unpolarized top decay and shall compare the polarized results in two different helicity systems. These predictions can be used to determine the polarization states of top quarks and also provide direct access to the B-hadron fragmentation functions (FFs) and allow us to deepen our knowledge of the hadronization process.

PACS numbers: 14.65.Ha, 14.40.Lb, 14.40.Nd, 13.88.+e, 12.38.Bx

Contents

1	Introduction	1
2	Angular structure of differential decay rate	3
3	Born approximation	4
4	Virtual one-loop corrections	5
5	QCD NLO contribution to angular distribution	6
6	Angular distribution results in Hadron level	10
7	Conclusion	13

1 Introduction

The top quark as a heaviest elementary particle, is the electroweak isospin partner of the bottom quark. Since its discovery by the CDF and *D0* experiments at Fermilab Tevatron[1], the determination of its properties has been one of the main goals of the Tevatron Collider, recently joined by the CERN Large Hadron Collider (LHC). The experiments at the LHC will allow one to perform improved measurements of the top properties, such as its total decay width Γ_t , mass m_t and branching fractions to high accuracy. The measurement of the top mass, as a fundamental parameter of the standard model (SM), has received particular attention. Indeed, the mass of top, the W -boson mass, and the Higgs boson mass are related through radiative corrections that provide an internal consistency check of the SM. In a recent paper [2], the mass of the top quark is measured as $m_t = 174.98 \pm 0.76$ GeV, by using the full sample of $p\bar{p}$ collision data collected by the *D0* experiment in Run II of the Fermilab Tevatron Collider at $\sqrt{s} = 1.96$ TeV. The theoretical aspects of top quark physics at the LHC are listed in [3].

The SM result of the top quark life time is $\tau_t \approx 0.5 \times 10^{-24}$ s [4] which is much shorter than the typical time for the formation of QCD bound states $\tau_{QCD} \approx 1/\Lambda_{QCD} \approx 3 \times 10^{-24}$ s, i.e. the top quark decays so rapidly that it does not have enough time to hadronize. Due to the Cabibbo-Kobayashi-Maskawa (CKM) mixing matrix element $V_{tb} \approx 1$ [5], the decay width of the top quark is dominated by the two-body channel $t \rightarrow b + W^+$ in the minimal SM of particle physics. At the top mass scale the strong coupling constant is small, $\alpha_s(m_t) \approx 0.1$, so that the QCD effects involving the top quark are well behaved in the perturbative sense. This allows one to apply the top quark decay as an appropriate tool for studying perturbative QCD and thus top decays provide a very clean source of information about the structure of the SM.

On the other hand, bottom quarks produced in the top decays hadronize before they decay and the bottom hadronization ($b \rightarrow B + X$) is indeed one of the sources of uncertainty in the measurement of the top mass at the LHC [6] and the Tevatron [7], as it contributes to the Monte Carlo systematics. At the LHC, recent studies [8] have suggested that final states with leptons, coming from the W^+ decay ($W^+ \rightarrow l^+ \nu_l$), and J/ψ , coming from the decay of a bottom-flavored meson (B), would be a promising channel to reconstruct the top mass. At the LHC, of particular interest is the distribution in the scaled-energy of B-meson (x_B) in the top quark rest frame as reliably as possible, so that this x_B distribution provides direct access to the B-hadron fragmentation functions (FFs). In [9], in addition to the x_B distribution, we also studied the doubly differential partial width $d^2\Gamma/(dx_B d\cos\theta)$ of the decay chain $t \rightarrow bW^+ \rightarrow Bl^+\nu_l + X$, where θ is the decay angle of the lepton in the W-boson rest frame. The $\cos\theta$ distribution allows one to analyze the W^+ -boson polarization and so to further constrain the B-meson FFs. In [10], we studied the QCD NLO corrections to the energy distribution of B-mesons from the decay of an unpolarized top quark into a stable charged-Higgs boson, $t \rightarrow BH^+ + X$, in the theories beyond-the-SM with an extended Higgs sector. Although, in [11] it is mentioned that there is a clear separation between the decays $t \rightarrow bW^+$ and $t \rightarrow bH^+$ at the LHC, in both the $t\bar{t}X$ pair production and the $t/\bar{t}X$ single top production.

The interplay between the top mass and its spin is of crucial importance in studying the SM. Due to the top large mass, the top quark decays rapidly so that its life time scale is much shorter than the typical time required for the QCD interactions to randomize its spin, therefore its full spin information is preserved in the decay and passes on to its decay products. Hence, the top quark polarization can be studied through the angular correlations between the direction of the top quark spin and the momenta of the decay products. Therefore, the particular purpose of this paper is to evaluate the QCD NLO corrections to the energy distribution of B-hadrons from the decay of a polarized top quark into a bottom quark, via $t(\uparrow) \rightarrow W^+ + b(\rightarrow B + X)$. We mention that highly polarized top quarks will become available at hadron colliders through single top production processes, which occur at the 33% level of the $t\bar{t}$ pair production rate [12], and in top quark pairs produced in future linear $e^+ - e^-$ -colliders [13]. In [14], we studied the angular distribution of the scaled-energy of the B/D-hadrons at NLO by calculating the polar angular correlation in the rest frame decay of a polarized top quark into a stable W^+ -boson and B/D-hadrons, via $t(\uparrow) \rightarrow W^+ + D/B + X$. We analyzed this angular correlation in a special helicity coordinate system with the event plane defined in the (x, z) plane and the z-axes along the b-quark momentum. In this frame (system 1), the top quark polarization vector was evaluated with respect to the direction of the b-quark momentum. Generally, to define the planes one needs to measure the momentum directions of the momenta \vec{p}_b and \vec{p}_W and the polarization direction of the top quark, where the measurement of the momentum direction of \vec{p}_b requires the use of a jet finding algorithm, whereas the polarization direction of the top quark must be obtained from the theoretical input. In electron-positron interactions the polarization degree of the top quark can be tuned with the help of polarized beams [15], so that a polarized linear electron-positron collider may be viewed as a copious source of close to zero and close to 100% polarized top quarks.

In the present work, we analyze the angular distribution of the B-hadron energy in a different helicity coordinate system where, as before, the event plane is the (x, z) plane but with the z -axis along the W^+ -boson. The polarization direction of the top quark is evaluated w.r.t this axes. This coordinate system (system 2) makes the calculations more complicated because of the presence of the W^+ -momentum $|\vec{p}_W|$ in the $\mathcal{O}(\alpha_s)$ real amplitude of the process $t \rightarrow b + W^+$. To obtain the scaled distribution of B-hadron energy, at first we present an analytical expression for the NLO corrections to the differential width of the decay process $t(\uparrow) \rightarrow b + W^+$ in two different helicity coordinate systems and then using the realistic and nonperturbative $b \rightarrow B$ FF we shall present and compare our results in both systems. The measurement of the energy distribution of the B-hadron will be important to deepen our understanding of the nonperturbative aspects of B-hadrons formation and to test the universality and scaling violations of the B-hadron FFs while the angular analysis of the polarized top decay constrain these FFs even further.

This paper is structured as follows. In Sec. 2, we introduce the angular structure of differential decay widths. In Secs. 3-5, we present our analytic results for the angular distributions of partial decay rates in two different helicity systems at the Born level and next-to-leading order by introducing the technical details of our calculations. In Sec. 6, we present our numerical analysis in hadron level and in Sec. 7, our conclusions are summarized.

2 Angular structure of differential decay rate

The dynamics of the current-induced $t \rightarrow b$ transition is embodied in the hadron tensor $H^{\mu\nu} \propto \sum_{X_b} \langle t(p_t, s_t) | J^{\mu\dagger} | X_b \rangle \langle X_b | J^\nu | t(p_t, s_t) \rangle$, where the SM current combination is given by $J_\mu = (J_\mu^V - J_\mu^A) \propto \bar{\psi}_b \gamma_\mu (1 - \gamma_5) \psi_t$, and s_t stands for the top quark spin. Here, the intermediate states are $|X_b \rangle = |b(p_b, s_b) \rangle$ for the Born term and virtual one-loop contributions and $|X_b \rangle = |b + g \rangle$ for the $\mathcal{O}(\alpha_s)$ real contributions.

In the rest frame of a top quark decaying into a b-quark, a W^+ -boson and a gluon, the final state particles b, W^+ and gluon define an event frame. Relative to this event plane one can define the polarization direction of the polarized top quark. There are two various choices of possible coordinate systems relative to the event plane where one differentiates between helicity systems according to the orientation of the z -axis. These systems are shown in Figs. 2 (system 1) and 3 (system 2). In the system 1, the three-momentum of the b-quark points into the direction of the positive z -axis and in the system 2, the momentum of the W -boson is defined along the positive z -axis.

Generally, the angular distribution of the differential decay width $d\Gamma/dx$ of a polarized top quark is expressed by the following form to clarify the correlation between the polarization of the top quark and its decay products

$$\frac{d^2\Gamma}{dx_i d\cos\theta_P} = \frac{1}{2} \left\{ \frac{d\Gamma_A}{dx_i} + P \frac{d\Gamma_B}{dx_i} \cos\theta_P \right\}, \quad (2.1)$$

where the polar angle θ_P shows the spin orientation of the top quark relative to the event plane and P is the magnitude of the top quark polarization. $P = 0$ stands for an unpolarized top quark while $P = 1$ corresponds to 100% top quark polarization. In the notation above,

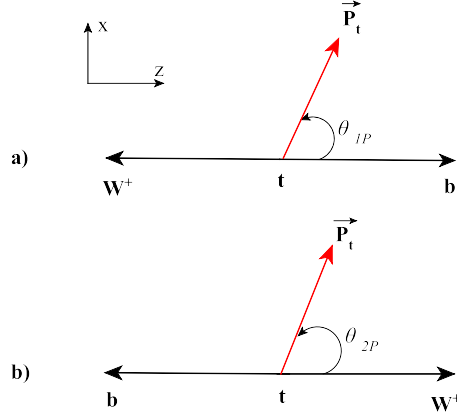


Figure 1. Definition of the polar angle θ_P in two helicity systems. \vec{P}_t is the top polarization vector.

$d\Gamma_A/dx$ and $d\Gamma_B/dx$ correspond to the unpolarized and polarized differential decay rates, respectively. As usual, we have defined the partonic scaled-energy fraction x_i as

$$x_i = \frac{2p_i \cdot p_t}{m_t^2}. \quad (2.2)$$

Neglecting the b -quark mass, one has $0 \leq x_i \leq 1 - \omega$ where ω is $\omega = m_W^2/m_t^2$. Throughout this paper, we use the normalized partonic energy fraction as

$$x_i = \frac{2E_i}{m_t(1 - \omega)}, \quad (i = b, g) \quad (2.3)$$

where E_i stands for the energy of outgoing partons (bottom or gluon) and $0 \leq x_i \leq 1$.

The $\mathcal{O}(\alpha_s)$ radiative corrections to the unpolarized differential rate $d\Gamma_A/dx$ have been studied in our previous work [9], extensively. The NLO radiative corrections to the polarized partial rate $d\Gamma_B/dx$ in the system 1 (Fig. 2) is studied in [14] by one of us. In the present work, we concentrate on the polarized top decay in the system 2 (Fig. 3) which is more complicated in comparison with the analysis performed in the system 1. Finally, we shall compare our results in two coordinate systems 1 and 2 at the hadron level.

3 Born approximation

It is straightforward to calculate the Born term contribution to the decay rate of the polarized top quark. The Born term tensor is obtained from the square of the Born amplitude, given by

$$M^{(0)} = V_{tb} \frac{g_W}{\sqrt{2}} \bar{u}_b \gamma^\mu \frac{1}{2} (1 - \gamma_5) u_t, \quad (3.1)$$

where g_W is related to the Fermi's constant G_F as $g_W/\sqrt{2} = 2m_W(G_F/\sqrt{2})^{1/2}$. After omitting the weak coupling factor $V_{tb}g_W/\sqrt{2}$ and summing over the b -quark spin, the Born term tensor reads

$$B^{\mu\nu} = \frac{1}{4} \text{Tr} \{ (\not{p}_b + m_b) \gamma^\mu (1 - \gamma_5) (\not{p}_t + m_t) (1 + \gamma_5 \not{S}_t) \gamma^\nu (1 - \gamma_5) \}. \quad (3.2)$$

Considering Fig. 1, we set the four-momentum and the polarization four-vector of the top quark as

$$p_t = (m_t; \vec{0}), \quad s_t = P(0; \sin \theta_P \cos \phi, \sin \theta_P \sin \phi, \cos \theta_P), \quad (3.3)$$

and in the coordinate system 1 (Fig. 1a), the four-momentum of the b-quark is set to $p_b = E_b(1; 0, 0, 1)$ and in the system 2 (Fig. 1b), it is $p_b = E_b(1; 0, 0, -1)$. Note that we put the b-quark mass to zero throughout this paper. Therefore, the Born term helicity structure of differential rates in the system 1, reads

$$\frac{d^2 \Gamma_1^{(0)}}{dx_b d \cos \theta_{1P}} = \frac{1}{2} \left\{ \Gamma_A^{(0)} - P \Gamma_B^{(0)} \cos \theta_{1P} \right\} \delta(1 - x_b), \quad (3.4)$$

and in the system 2, is expressed as

$$\frac{d^2 \Gamma_2^{(0)}}{dx_b d \cos \theta_{2P}} = \frac{1}{2} \left\{ \Gamma_A^{(0)} + P \Gamma_B^{(0)} \cos \theta_{2P} \right\} \delta(1 - x_b), \quad (3.5)$$

where, $\Gamma_A^{(0)}$ corresponds to the unpolarized Born term rate and $\Gamma_B^{(0)}$ describes the polarized Born rate. They are given by

$$\Gamma_A^{(0)} = \frac{\sqrt{2} m_t^3 G_F}{16\pi} (1 + 2\omega)(1 - \omega)^2, \quad \Gamma_B^{(0)} = \frac{\sqrt{2} m_t^3 G_F}{16\pi} (1 - 2\omega)(1 - \omega)^2. \quad (3.6)$$

These results are in agreement with Refs. [16] and [17]. Setting $m_W = 80.399$ GeV, $m_t = 174.98$ GeV and $G_F = 1.16637 \times 10^{-5}$ GeV⁻² one has $\Gamma_A^{(0)} = 1.4335$ and $\Gamma_B^{(0)} = 0.5939$. Therefore, the polarization asymmetry α_W , which is defined as $\alpha_W = \Gamma_B^{(0)} / \Gamma_A^{(0)}$, is $\alpha_W = 0.396$.

4 Virtual one-loop corrections

The required ingredients for the NLO calculation are the virtual one-loop contributions and the tree-graph contributions. Since at the one-loop level, QED and QCD have the same structure then the virtual one-loop corrections to the fermionic left-chiral (V-A) transitions have a long history, even dates back to QED times.

The virtual one-loop contributions into the polarized differential width are the same in both helicity systems 1 and 2, and can be found in [14]. We just mention that the virtual corrections arise from a virtual gluon exchanged between the top and bottom quark legs (vertex correction), and from emission and absorption of a virtual gluon from the same quark leg (quark self energy). Both of them include the IR and UV singularities, which are regularized by dimensional regularization in D space-time dimensions, where $D = 4 - 2\epsilon$. All UV divergences are canceled after summing all virtual contributions up, whereas the IR singularities are remaining, which are labeled by ϵ from now on. Therefore, following the general form of the doubly differential distribution (2.1), the virtual contribution in both coordinate systems is

$$\frac{d^2 \Gamma^{\text{vir}}}{dx_b d \cos \theta_P} = \frac{1}{2} \left\{ \frac{d\Gamma_A^{\text{vir}}}{dx_b} + P \frac{d\Gamma_B^{\text{vir}}}{dx_b} \cos \theta_P \right\}, \quad (4.1)$$

where

$$\begin{aligned}\frac{d\Gamma_A^{\text{vir}}}{dx_b} &= \Gamma_A^{(0)} \frac{C_F \alpha_s}{2\pi} \left\{ R - 4 \frac{1-\omega}{1-4\omega^2} \ln(1-\omega) \right\} \delta(1-x_b), \\ \frac{d\Gamma_B^{\text{vir}}}{dx_b} &= \Gamma_B^{(0)} \frac{C_F \alpha_s}{2\pi} R \delta(1-x_b).\end{aligned}\tag{4.2}$$

In the equations above, R is defined as

$$R = -\frac{F^2}{2} + \frac{F}{\epsilon} - \frac{1-4\omega}{1-2\omega} \ln(1-\omega) + 2 \ln \omega \ln(1-\omega) + 2 Li_2(1-\omega) - \frac{1}{\epsilon^2} - 5 \frac{\pi^2}{12} - \frac{23}{8},\tag{4.3}$$

where, $F = 2 \ln(1-\omega) - \ln(4\pi\mu_F^2/m_t^2) + \gamma_E - \frac{5}{2}$. Here, $\gamma_E = 0.5772 \dots$ is the Euler Mascheroni constant, $Li_2(x)$ is the known dilogarithmic function and μ_F is the QCD scale parameter. The one-loop virtual contribution is purely real, as can be found from an inspection of the one-loop Feynman diagrams, which does not accept any nonvanishing physical two-particle cut.

5 QCD NLO contribution to angular distribution

At $\mathcal{O}(\alpha_s)$, the full amplitude of the transition $t \rightarrow b$ is the sum of the amplitudes of the Born term, virtual one-loop and the real gluon (tree-graph) contributions

$$M = M^{(0)} + M^{\text{loop}} + M^{\text{real}},\tag{5.1}$$

where, the real amplitude results from the decay $t(p_t) \rightarrow b(p_b) + W^+(p_W) + g(p_g)$, as

$$\begin{aligned}M^{\text{real}} &= e g_s \frac{T_{ij}^n}{2\sqrt{2} \sin \theta_W} \epsilon_\beta^*(p_g, s_g) \epsilon_\mu(p_W, s_W) \bar{u}(p_b, s_b) \left\{ \gamma^\beta \frac{\not{p}_g + \not{p}_b}{2p_b \cdot p_g} \gamma^\mu (1 - \gamma_5) - \right. \\ &\quad \left. \gamma^\mu (1 - \gamma_5) \frac{m_t + \not{p}_t - \not{p}_g}{2p_t \cdot p_g} \gamma^\beta \right\} u(p_t, s_t).\end{aligned}\tag{5.2}$$

Here, $g_s = \sqrt{4\pi\alpha_s}$ is the strong coupling constant, the angle θ_W is the weak mixing angle so that $\sin^2 \theta_W = 0.23124$ [18], and "n" is the color index so $Tr(T^n T^n)/3 = C_F$. The polarization vectors of the gluon and the W -boson are also denoted by $\epsilon(p, s)$.

The QCD NLO contribution results from the square of the full amplitude as

$$|M|^2 = |M^{(0)}|^2 + |M^{\text{vir}}|^2 + |M^{\text{real}}|^2 + \mathcal{O}(\alpha_s^2),\tag{5.3}$$

where, $|M^{\text{vir}}|^2 = 2M^{(0)\dagger} M^{\text{loop}}$ and $|M^{\text{real}}|^2 = M^{\text{real}\dagger} M^{\text{real}}$. To regulate the IR singularities, which arise from the soft- and collinear-gluon emission, we work in D-dimensions approach in which to extract divergences we take the following replacement

$$\int \frac{d^4 p}{(2\pi)^4} \rightarrow \mu^{4-D} \int \frac{d^D p}{(2\pi)^D},\tag{5.4}$$

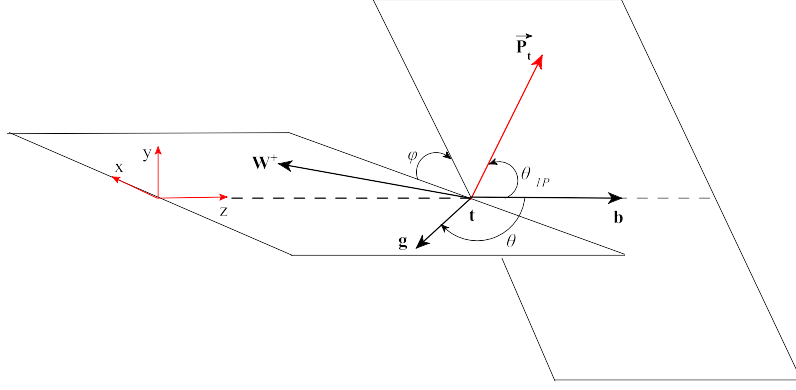


Figure 2. Definition of the azimuthal angle ϕ , the polarization vector of the top quark \vec{P}_t , the polar angles θ and θ_P in the helicity coordinate system 1.

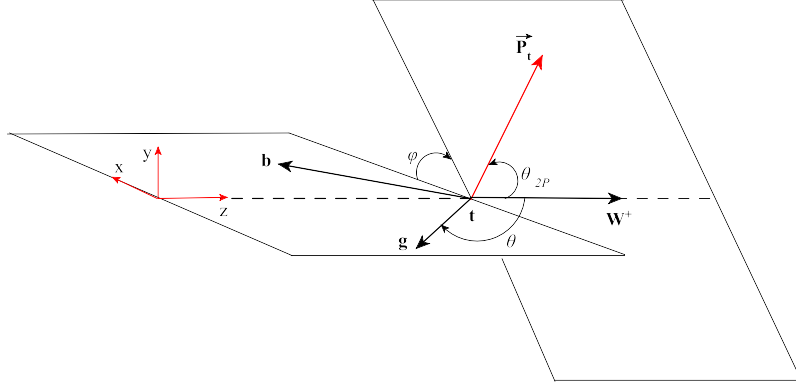


Figure 3. As in Fig. 2, but in the helicity coordinate system 2.

where, μ is an arbitrary reference mass which shall be removed after summing all corrections up. The differential decay rate for the real contribution is given by

$$d\Gamma^{\text{real}} = \frac{\mu_F^{2(4-D)}}{2m_t} |\overline{M^{\text{real}}}|^2 dR_3(p_t, p_b, p_g, p_W), \quad (5.5)$$

where, the 3-body phase space element dR_3 reads

$$dR_3 = \frac{d^{D-1}\mathbf{p}_b}{(2\pi)^{D-1}2E_b} \frac{d^{D-1}\mathbf{p}_W}{(2\pi)^{D-1}2E_W} \frac{d^{D-1}\mathbf{p}_g}{(2\pi)^{D-1}2E_g} (2\pi)^D \delta^D(p_t - p_b - p_W - p_g). \quad (5.6)$$

To calculate the real doubly differential rate $d^2\Gamma^{\text{real}}/(dx_b d\cos\theta_P)$ and to get the correct finite terms, we normalize the polarized and the unpolarized doubly differential distributions to the corresponding Born widths evaluated in D-dimensions. The polarized and unpolarized Born widths $\Gamma_B^{(0)}$ and $\Gamma_A^{(0)}$, evaluated in the dimensional regularization at $\mathcal{O}(\epsilon^2)$ are given in Eq. (29) of Ref. [14]. Following Eq. (2.1), the $\mathcal{O}(\alpha_s)$ corrections to the angular distribution of partial decay rates are obtained by summing the Born, the virtual and real

gluon contributions and is given by

$$\frac{d^2\Gamma^{\text{nlo}}}{dx_b d\cos\theta_P} = \frac{1}{2} \left\{ \frac{d\Gamma_A^{\text{nlo}}}{dx_b} + P \frac{d\Gamma_B^{\text{nlo}}}{dx_b} \cos\theta_P \right\}. \quad (5.7)$$

Generally, the contribution of the real gluon emission depends on the various choices of possible coordinate systems. The results for $d\Gamma_A^{\text{nlo}}/dx_b$ are the same in both helicity systems and can be found in [9], and the analytical expression of the polarized angular distribution of decay width in the helicity system 1 ($d\Gamma_{1B}^{\text{nlo}}/dx_b$) is presented in [14].

To calculate the real differential rate $d\Gamma^{\text{real}}/dx_b$ in the coordinate system 2, we fix the momentum of b-quark and integrate over the energy of the W -boson which ranges from $E_W^{\text{min}} = m_t(\omega + [1 - x_b(1 - \omega)]^2)/(2[1 - x_b(1 - \omega)])$ to $E_W^{\text{max}} = m_t(1 + \omega)/2$, and to evaluate the angular distribution of differential width $d^2\Gamma^{\text{real}}/(dx_b d\cos\theta_{2P})$, the angular integral in D -dimensions will have to be written as

$$d\Omega_W = -\frac{2\pi^{\frac{D}{2}-1}}{\Gamma(\frac{D}{2}-1)} (\sin\theta_{2P})^{D-4} d\cos\theta_{2P}. \quad (5.8)$$

Therefore, the doubly differential distribution reads

$$\frac{d^2\Gamma_2^{\text{real}}}{dx_b d\cos\theta_{2P}} \propto x_b^{D-4} \overline{|M^{\text{real}}|^2} (1 - \cos^2\alpha)^{\frac{D-4}{2}} \delta(\cos\alpha - b) dE_W d\cos\alpha, \quad (5.9)$$

where, $b = (m_t^2 + m_W^2 - 2m_t(E_b + E_W) + 2E_b E_W)/(2E_b p_W)$, the coefficient of proportionality reads $\mu_F^{2(4-D)} (p_W m_t)^{D-4} (1 - \omega)^{D-3} / (2^{3D-4} \pi^{D-1} \Gamma^2(\frac{D}{2} - 1))$, $p_W = \sqrt{E_W^2 - m_W^2}$ is the momentum of W -boson and α is the angle between the b-quark and the W -boson in Fig. 3. Due to the presence of the W -momentum, working in the helicity system 2 is more complicated than the system 1 and for this reason our analytical results will not appear in a dinky form as in system 1 (see Eq. (35) in [14]).

Considering the top rest frame, the relevant scalar products evaluated in the system 2, are

$$p_W \cdot s_t = -P p_W \cos\theta_{2P}, \quad p_b \cdot s_t = -P E_b \cos\alpha \cos\theta_{2P}, \quad p_b \cdot p_W = E_b(E_W - p_W \cos\alpha), \quad (5.10)$$

and $p_t \cdot s_t = 0$. Here, P refers to the polarization degree of the top quark. To obtain the analytic result for the angular distribution of the differential rate at NLO, by summing the Born level, the virtual and real gluon contributions, one has

$$\frac{d\Gamma_{2B}^{\text{nlo}}}{dx_b} = \Gamma_B^{(0)} \left\{ \delta(1 - x_b) + \frac{C_F \alpha_s}{2\pi} \left\{ \left[-\frac{1}{\epsilon} + \gamma_E - \ln 4\pi \right] \left[\frac{3}{2} \delta(1 - x_b) + \frac{1 + x_b^2}{(1 - x_b)_+} \right] + T_1 \right\} \right\}, \quad (5.11)$$

where,

$$\begin{aligned}
T_1 = & \delta(1-x_b) \left\{ -\frac{3}{2} \ln \frac{\mu_F^2}{m_t^2} + \frac{2(1-\omega)}{1-2\omega} \ln(1-\omega) - \frac{2\pi^2}{3} - \frac{2\omega}{1-\omega} \ln \omega + 2 \ln \omega \ln(1-\omega) + \right. \\
& 4Li_2(1-\omega) - 6 \left. \right\} + 2(1+x_b^2) \left(\frac{\ln(1-x_b)}{1-x_b} \right)_+ + \frac{1}{(1-x_b)_+} \left\{ 2(1+x_b^2) \ln \frac{m_t x_b (1-\omega)}{\mu_F} \right. \\
& + (1-x_b) \left[(1-x_b)(1-2x_b) - \frac{4x_b}{1-\omega} \right] - 2x_b^2 \left. \right\} - \frac{2(1+x_b^2)}{1-x_b} \ln(1-x_b) \\
& - 2(2+x_b+x_b^2) + \frac{1}{(1-\omega)(1-2\omega)} \left\{ 2(1-3\omega) - 4x_b(\omega^2+\omega-1) - \frac{4\omega(1-2\omega)}{1-x_b} - \right. \\
& \frac{4(1-\omega)}{(1-x_b(1-\omega))(\omega x_b^2 - (2-x_b)^2)} \left\{ (1-\omega-\omega^2)x_b^2 + 2 + \frac{-4\omega^3+5\omega-3}{1-\omega} x_b \right\} \left. \right\} \\
& - \left(H - 2 \ln(1-x_b) \right) \sqrt{\frac{(2-x_b)^2 - \omega x_b^2}{1-\omega}} \left\{ \frac{1}{(2-x_b)^2 - \omega x_b^2} \left\{ \frac{2(4\omega x_b - 6\omega + 5)}{1-2\omega} - \right. \right. \\
& \left. \left. \frac{4}{(1-\omega)(1-2\omega)} + (x_b(1+\omega) - 2) \left(1 - \frac{2(1+\omega)}{(1-\omega)(\omega x_b^2 - (2-x_b)^2)} \right) \right\} + 1 - \frac{2}{1-x_b} \right\}, \tag{5.12}
\end{aligned}$$

where $H = \ln \left(2S^2 x_b^4 + 4S(1-x_b)x_b^2 + 2x_b(-Sx_b^2 + x_b - 1) \sqrt{S(x_b(Sx_b - 2) + 2)} + (1-x_b)^2 \right)$ and $S = (1-\omega)/2$.

Since the detected mesons in top decays can be also produced through a fragmenting real gluon, therefore, to obtain the most accurate energy spectrum of B-meson we have to add the contribution of gluon fragmentation to the b-quark one to produce the outgoing meson. As shown in [14], this contribution can be important at a low energy of the observed meson so that this decreases the size of decay rate at the threshold. Therefore, the angular distribution of the differential decay rate $d\Gamma/dx_g$ is also required, where x_g is defined in (2.3). Considering the general form of the angular distribution (2.1), for the gluon contribution one has

$$\frac{d^2\Gamma^{\text{nlo}}}{dx_g d\cos\theta_P} = \frac{1}{2} \left\{ \frac{d\Gamma_A^{\text{nlo}}}{dx_g} + P \frac{d\Gamma_B^{\text{nlo}}}{dx_g} \cos\theta_P \right\}, \tag{5.13}$$

where, the results for $d\Gamma_A^{\text{nlo}}/dx_g$ are the same in both coordinate systems and can be found in [9], and the analytical expression for the polarized angular distribution in the helicity system 1 ($d\Gamma_{1B}^{\text{nlo}}/dx_g$) is presented in [14]. In the system 2, to obtain the doubly differential distribution $d^2\Gamma/(dx_g d\cos\theta_{2P})$ we fix the momentum of the gluon and integrate over the energy of W-boson which ranges from $E_W^{\text{min}} = m_t(\omega + [1-x_g(1-\omega)]^2)/(2[1-x_g(1-\omega)])$ to $E_W^{\text{max}} = m_t(1+\omega)/2$. Therefore, the doubly differential decay rate is given by

$$\frac{d^2\Gamma_2^{\text{real}}}{dx_g d\cos\theta_{2P}} \propto x_g^{D-4} |M^{\text{real}}|^2 (1 - \cos^2\theta)^{\frac{D-4}{2}} \delta(\cos\theta - a) dE_W d\cos\theta, \tag{5.14}$$

where, the proportionality coefficient is as in (5.9), θ is the polar angle between the gluon and the W-boson (see Fig. 3), whereas $a = (m_t^2 + m_W^2 - 2m_t(E_g + E_W) + 2E_g E_W)/(2E_g p_W)$.

The relevant scalar products are

$$p_W \cdot s_t = -P p_W \cos \theta_{2P}, \quad p_g \cdot s_t = -P E_g \cos \theta \cos \theta_{2P}, \quad p_g \cdot p_W = E_g(E_W - p_W \cos \theta). \quad (5.15)$$

Therefore, in the coordinate system 2 the polarized differential width is expressed as

$$\frac{d\Gamma_{2B}^{\text{nlo}}}{dx_g} = \Gamma_B^{(0)} \frac{C_F \alpha_s}{2\pi} \left\{ \frac{1 + (1 - x_g)^2}{x_g} \left(-\frac{1}{\epsilon} + \gamma_E - \ln 4\pi \right) + T_2 \right\} \quad (5.16)$$

where,

$$\begin{aligned} T_2 = & \frac{1 + (1 - x_g)^2}{x_g} \left\{ 2 \ln \frac{m_t x_g (1 - \omega)}{\mu_F} - \ln(1 - x_g(1 - \omega)) \right\} - \\ & \frac{\omega}{2(1 - x_g(1 - \omega))^2} \left\{ 2 + \frac{8\omega}{(1 - \omega)(1 - 2\omega)} - \frac{x_g(6\omega^2 + \omega + 2)}{1 - 2\omega} \right\} + \\ & \frac{\ln(1 - x_g(1 - \omega))}{1 - \omega} \left\{ \frac{2(1 + 2\omega)}{1 - 2\omega} - \frac{2(1 + 4\omega)}{x_g(1 - \omega)(1 - 2\omega)} + \frac{2(1 + \omega^2)}{x_g^2(1 - \omega)^2} \right\} \\ & - \frac{1}{1 - 2\omega} \left\{ 1 + \frac{2(1 + \omega)^2}{1 - \omega} + \frac{x_g}{2}(2\omega - 5) \right\} + \frac{4\omega}{x_g(1 - \omega)^2}. \end{aligned} \quad (5.17)$$

In Eqs. (5.11) and (5.16), T_1 and T_2 are free of all singularities and to subtract the collinear singularities remaining in the polarized partial widths, we apply the modified minimal-subtraction (\overline{MS}) scheme where, the singularities are absorbed into the bare FFs. This renormalizes the FFs and creates the finite terms of the form $\alpha_s \ln(m_t^2/\mu_F^2)$ in the the polarized differential widths. According to this scheme, to get the \overline{MS} coefficient functions one shall has to subtract from Eqs. (5.11) and (5.16), the $\mathcal{O}(\alpha_s)$ term multiplying the characteristic \overline{MS} constant $(-1/\epsilon + \gamma_E - \ln 4\pi)$. In the present work we set $\mu_F = m_t$, so that the terms proportional to $\ln(m_t^2/\mu_F^2)$ vanish.

We mention that the dimensional reduction scheme can be converted to the gluon mass regulator scheme by the replacement $1/\epsilon - \gamma_E + \ln(4\pi\mu_F^2/m_t^2) \rightarrow \ln \Lambda^2$, where $\Lambda = m_g/m_t$ is the scaled gluon mass.

6 Angular distribution results in Hadron level

After determination of the differential decay rates in the parton level, we are now in a position to explore our phenomenological predictions of the energy distribution of B-meson by performing a numerical analysis in the two helicity coordinate systems. In fact, we wish to calculate the quantity $d\Gamma/dx_B$, where the normalized energy fraction of the outgoing meson is defined as $x_B = 2E_B/(m_t(1 - \omega))$, in similarity to the parton level one (2.3). The necessary tool to obtain the B-meson energy spectrum is the factorization theorem of the QCD-improved parton model [19], where the energy distribution of a hadron is expressed as the convolution of the parton-level spectrum with the nonperturbative FF $D_i^B(z, \mu_F)$

$$\frac{d\Gamma}{dx_B} = \sum_{i=b,g} \int_{x_i^{\min}}^{x_i^{\max}} \frac{dx_i}{x_i} \frac{d\Gamma_i}{dx_i}(\mu_R, \mu_F) D_i\left(\frac{x_B}{x_i}, \mu_F\right), \quad (6.1)$$

where, $d\Gamma_i/dx_i$ is the partial width of the parton-level process $t \rightarrow i(=b, g) + X$, with X including the W -boson and any other parton. Here, μ_F and μ_R are the factorization and the renormalization scales, respectively, that the scale μ_R is associated with the renormalization of the strong coupling constant and a normal choice, which we adopt in this work is $\mu_R = \mu_F = m_t$. In (6.1), $D_{i=b,g}(z, \mu_F)$ is the nonperturbative FF of the transition $b/g \rightarrow B$ which is process independent. It means, we can exploit data from $e^+e^- \rightarrow b\bar{b}$ processes to predict the b-quark hadronization in top decay. Note that the definitions of $d\Gamma/dx_i$ and $D_i^B(z, \mu_F)$ are not unique, but they depend on the scheme which is used to subtract the collinear singularities appeared in the differential widths (5.11) and (5.16). As we mentioned, in our work the \overline{MS} factorization scheme is chosen.

Several models, including some fittable parameters have been already proposed to describe the nonperturbative transition from a quark- to a hadron-state. Following Ref. [20], we employ the B-hadron FFs determined at NLO in the zero-mass scheme, through a global fit to e^+e^- -annihilation data presented by ALEPH [21] and OPAL [22] collaborations at CERN LEP1 and by SLD [23] at SLAC SLC. Specifically, at the initial scale $\mu_0 = m_b$ the power model $D_b^B(z, \mu_0) = Nz^\alpha(1-z)^\beta$ is proposed for the $b \rightarrow B$ transition, while the gluon FF is set to zero and is evolved to higher scales using the Dokshitzer-Gribov-Lipatov-Altarelli-Parisi (DGLAP) equations [24]. The results for the fit parameters are $N = 4684.1, \alpha = 16.87$ and $\beta = 2.628$. As numerical input values, from [18] we take $G_F = 1.16637 \times 10^{-5} \text{ GeV}^{-2}$, $m_W = 80.339 \text{ GeV}$, $m_b = 4.78 \text{ GeV}$, $m_B = 5.279 \text{ GeV}$, and the typical QCD scale $\Lambda_{\overline{MS}}^{(5)} = 231.0 \text{ MeV}$ adjusted such that $\alpha_s^{(5)}(m_Z = 91.18) = 0.1184$. In the \overline{MS} scheme the b-quark mass only enter through the initial condition of the FF.

Before studying the B-hadron spectrum, we turn to our numerical results of the unpolarized and polarized decay rates in both helicity systems. In fact, we integrate $d\Gamma/dx_b$ (Eqs. (5.11), (35) from [14] and (7) from [9]) over $x_b(0 \leq x_b \leq 1)$, while the strong coupling constant is evolved from $\alpha_s(m_Z) = 0.1184$ to $\alpha_s(m_t) = 0.1070$. The normalized result for the polarized decay width in the helicity system 1 is

$$\frac{\Gamma_{1B}^{\text{nlo}}}{\Gamma_B^{(0)}} = 1 - 0.1303, \quad (6.2)$$

and for the one in the system 2, is

$$\frac{\Gamma_{2B}^{\text{nlo}}}{\Gamma_B^{(0)}} = 1 - 0.2814, \quad (6.3)$$

and the unpolarized decay rate normalized to the corresponding Born term, is

$$\frac{\Gamma_A^{\text{nlo}}}{\Gamma_A^{(0)}} = 1 - 0.08542. \quad (6.4)$$

To study the x_B scaled-energy distributions of B-hadrons produced in the polarized top decay, we consider the quantity $d\Gamma(t(\uparrow) \rightarrow B + X)/dx_B$ in the two helicity coordinate systems. In [9, 14], we showed that the $g \rightarrow B$ contribution into the NLO energy spectrum of the B-meson is negative and appreciable only in the low- x_B region and for higher values of

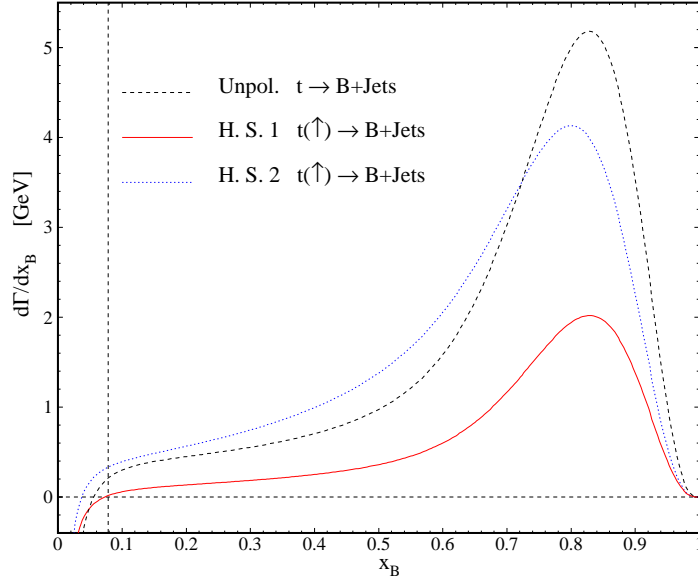


Figure 4. $d\Gamma_B^{\text{nlo}}/dx_B$ as a function of x_B in the helicity system 1 (solid line) and the system 2 (dotted line). The polarized results are also compared to the unpolarized one $d\Gamma_A^{\text{nlo}}/dx_B$ (dashed line). Threshold at x_B is shown.

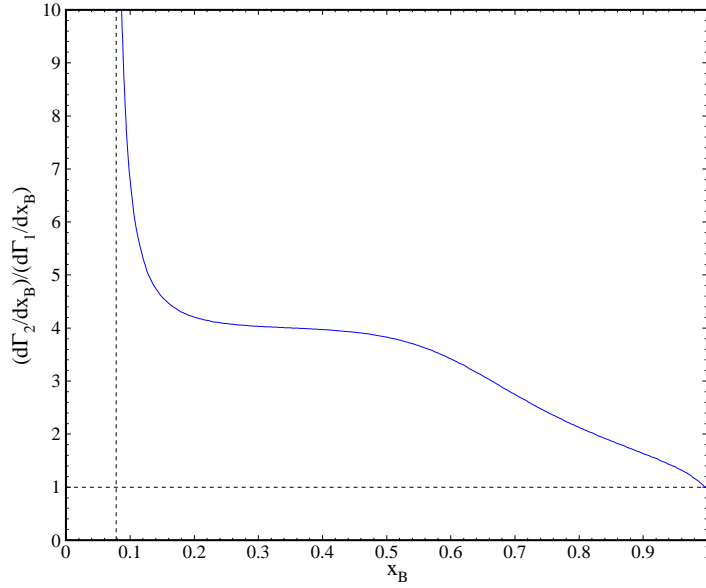


Figure 5. x_B spectrum at NLO in the helicity system 2, normalized to the one in the system 1.

x_B the NLO result is practically exhausted by the $b \rightarrow B$ contribution. The contribution of the gluon is calculated to see where it contributes to $d\Gamma/dx_B$ and can not be discriminated in the meson spectrum as an experimental quantity.

In Fig. 4, the x_B -spectrum of the B-hadron produced in the unpolarized top quark

decay (dashed line) is shown. The polarized ones in the helicity system 1 (solid line) and system 2 (dotted line) are also studied. As is seen, the differential decay width of the polarized top in the helicity system 2 (H. S. 2) is totally higher than the one in the helicity system 1 (H. S. 1). For a more quantitative interpretation of Fig. 4, we consider in Fig. 5 the partial decay width $d\Gamma_B^{\text{plo}}/dx_b$ in the H. S. 2 normalized to the one in the H. S. 1. Note that all results are valid just for $x_B \geq 2m_B/(m_t(1 - \omega)) = 0.078$.

7 Conclusion

Studying the fundamental properties of the top quark is one of the main fields of investigation in theoretical and experimental particle physics. The short life time of the top quark implies that it decays before hadronization takes place; therefore, it retains its full polarization content and passes on the spin information to its decay products. This allows us to study the top-spin state using the angular distributions of its decay products. Whereas the bottom quark, produced through the top decay, hadronizes therefore the distributions in the B-hadron energy are of particular interest. In [9], we studied the scaled-energy distribution of the B-meson in unpolarized top quark decays $t \rightarrow W^+ + b(\rightarrow B)$. In [14], we made our predictions for the scaled-energy distributions of the B- and D-mesons from polarized top decays using a special helicity coordinate system, where the event plane lies in the (x, z) plane and the bottom momentum is along the z -axis. In the present work, we have presented results on the $\mathcal{O}(\alpha_s)$ radiative corrections to the spin dependent differential width $d^2\Gamma/(dx_B d\cos\theta_P)$, applying a different helicity system where the z -axis is defined by the W -momentum. This provides independent probes of the polarized top quark decay dynamics. To obtain these results we presented, for the first time, the analytical results for the parton-level differential decay widths of $t \rightarrow b + W^+$ in two helicity systems and then we compared our results in both systems. We found that the polarized results depend on the selected helicity system, extremely.

On one hand, the x_B distributions provide direct access to the B-hadron FFs, and on the other hand the universality and scaling violations of the B-hadron FFs will be able to test at LHC by comparing our predictions with future measurements of $d\Gamma/dx_B$. The $\cos\theta_P$ distribution allows one to analyze the polarization state of top quarks, where the polar angle θ_P refers to the angle between the top polarization vector and the z -axis. The formalism made here is also applicable to the other hadrons such as pions and kaons, using the $(b, g) \rightarrow (\pi, K)$ FFs which can be found in [25].

Acknowledgments

We would like to thank Professor B. A. Kniehl for reading the manuscript and also for his important comments. S. M. Moosavi Nejad thanks the CERN TH-PH division for its hospitality, where a portion of this work was performed. Thanks to Z. Hamedani for reading and improving the English manuscript.

References

- [1] Tevatron EW Working Group and CDF & D0 Collaboration, arXiv:0903.2503 [hep-ex].
- [2] V. M. Abazov *et al.* [D0 Collaboration], Phys. Rev. Lett. **113** (2014) 032002 [arXiv:1405.1756 [hep-ex]].
- [3] W. Bernreuther, J. Phys. G **35**, 083001 (2008).
- [4] K. G. Chetyrkin, R. Harlander, T. Seidensticker and M. Steinhauser, Phys. Rev. D **60** (1999) 114015 [hep-ph/9906273].
- [5] N. Cabibbo, Phys. Rev. Lett. **10**, 531 (1963); M. Kobayashi and T. Maskawa, Prog. Theor. Phys. **49**, 652 (1973).
- [6] M. Beneke, I. Efthymiopoulos, M.L. Mangano, J. Womersley *et al.*, in Proceedings of 1999 CERN Workshop on Standard Model Physics (and more) at the LHC, CERN 2000-004, G. Altarelli and M.L. Mangano eds., p. **419**, [hep-ph/0003033].
- [7] A. Abulencia *et al.* [CDF Collaboration], Phys. Rev. Lett. **96** (2006) 022004; V. M. Abazov *et al.* [D0 Collaboration], Phys. Lett. B **606** (2005) 25.
- [8] A. Kharchilava, Phys. Lett. B **476** (2000) 73 [hep-ph/9912320].
- [9] B. A. Kniehl, G. Kramer and S. M. M. Nejad, Nucl. Phys. B **862**, 720 (2012) arXiv:1205.2528 [hep-ph].
- [10] S. M. Moosavi Nejad, Phys. Rev. D **85**, 054010 (2012); S. M. Moosavi Nejad, Eur. Phys. J. C **72** (2012) 2224 [arXiv:1205.6139 [hep-ph]].
- [11] A. Ali, F. Barreiro and J. Llorente, Eur. Phys. J. C **71**, 1737 (2011).
- [12] G. Mahlon and S. J. Parke, Phys. Rev. D **55**, 7249 (1997).
- [13] J. H. Kühn, Nucl. Phys. B **237**, 77 (1984); J. H. Kühn, A. Reiter and P. M. Zerwas, Nucl. Phys. B **272**, 560 (1986); S. Groote and J. G. Körner, Z. Phys. C **72** (1996) 255 [Erratum-ibid. C **70** (2010) 531].
- [14] S. M. M. Nejad, Phys. Rev. D **88** (2013) 9, 094011 [arXiv:1310.5686 [hep-ph]].
- [15] S. J. Parke and Y. Shadmi, Phys. Lett. B **387** (1996) 199 [hep-ph/9606419].
- [16] M. Fischer, S. Groote, J. G. Körner and M. C. Mauser, Phys. Rev. D **65**, 054036 (2002).
- [17] M. Fischer, S. Groote, J. G. Körner, M. C. Mauser and B. Lampe, Phys. Lett. B **451**, 406 (1999).
- [18] K. Nakamura *et al.* (Particle Data Group), J. Phys. G **37**, 075021 (2010).
- [19] J. C. Collins, Phys. Rev. D **66** (1998) 094002.
- [20] B. A. Kniehl, G. Kramer, I. Schienbein and H. Spiesberger, Phys. Rev. D **77**, 014011 (2008).
- [21] A. Heister *et al.* (ALEPH Collaboration), Phys. Lett. B **512**, 30 (2001).
- [22] G. Abbiendi *et al.* (OPAL Collaboration), Eur. Phys. J. C **29**, 463 (2003).
- [23] K. Abe *et al.* (SLD Collaboration), Phys. Rev. Lett. **84**, 4300 (2000); Phys. Rev. D **65**, 092006 (2002).
- [24] V. N. Gribov and L. N. Lipatov, Sov. J. Nucl. Phys. **15**, 438 (1972) [Yad. Fiz. **15**, 781 (1972)]; G. Altarelli and G. Parisi, Nucl. Phys. **B126**, 298 (1977); Yu. L. Dokshitzer, Sov. Phys. JETP **46**, 641 (1977) [Zh. Eksp. Teor. Fiz. **73**, 1216 (1977)].

- [25] M. Soleymaninia, A. N. Khorramian, S. M. Moosavinejad and F. Arbabifar, Phys. Rev. D **88**, 054019 (2013).